https://doi.org/10.5194/bg-2019-292
Preprint. Discussion started: 7 August 2019

Biogeosciences Discussions
Open Access

DRIFTS peaks as measured pool size proxy to reduce parameter uncertainty of soil organic matter models

Moritz Laub[1], Michael Scott Demyan[2], Yvonne Funkuin Nkwain[1], Sergey Blagodatsky[1], Thomas Kätterer[3], Hans-Peter Piepho[4], Georg Cadisch [1]

[1] Institute of Agricultural Sciences in the Tropics (Hans-Ruthenberg-Institute), University of Hohenheim, 70599 Stuttgart, Garbenstrasse 13, Germany

[2] School of Environment and Natural Resources, The Ohio State University, Columbus, 2021 Coffey Rd., OH, USA, 43210

[3] Department of Ecology, Swedish University of Agricultural Sciences, Uppsala, Ulls Väg 16, Sweden

[4] Institute of Biostatistics, University of Hohenheim, 70599 Stuttgart, Fruwirthstr. 23, Germany

Correspondence to: Moritz Laub (moritz.laub@uni-hohenheim.de)

Abbreviations: soil organic matter (SOM), Diffuse reflectance mid infrared Fourier transform spectroscopy (DRIFTS), DRIFTS stability index (DSI), soil microbial biomass carbon (SMB-C), squared model error (SME), soil organic carbon (SOC)

Abstract. The initialization of soil organic matter (SOM) turnover models has been a challenge for decades. Instead of using laborious and error prone size-density fractionation SOM pool partitioning, we propose the inexpensive, rapid, and non-destructive Diffuse reflectance mid infrared Fourier transform spectroscopy (DRIFTS) technique on bulk soil samples to gain information on SOM pool partitioning from the spectra. Specifically, the DRIFTS stability index, defined as the ratio of aliphatic C-H (2930 cm^{-1}) to aromatic C=C (1620 cm^{-1}) stretching vibrations, was used to divide SOM into fast and slow cycling pools in the soil organic module of the DAISY model. Long-term bare fallow plots from Bad Lauchstädt (Chernozem, 25 years) and the Ultuna frame trial in Sweden (Cambisol, 50 years) were combined with bare fallow plots of 7 years duration in the Kraichgau and Swabian Jura region in Southwest Germany (Luvisols). All fields had been in agricultural use for centuries before fallow establishment, so classical theory would suggest an initial steady state of SOM, which was hence used to compare the performance of DAISY initializations against the newly established DRIFTS stability index. The test was done using two different published parameter sets ($2.7 * 10^{-6}$ d^{-1}, $1.4 * 10^{-4}$ d^{-1}, 0.1 compared to $4.3 * 10^{-5}$ d^{-1}, $1.4 * 10^{-4}$ d^{-1}, 0.3 for the turnover rates of slow pool, fast pool and humification efficiency, respectively). The DRIFTS initialization of SOM pools significantly reduced model errors of poor performing model runs assuming steady state, irrespective of the turnover rates used, but the faster turnover parameter set fit better to all sites except Bad Lauchstädt. This suggests that soils under long-term agricultural use were not necessarily at steady state. A Bayesian calibration was applied in a next step to identify the best-fitting turnover rates for the DRIFTS stability index in DAISY, both for each site individually and for a combination of all sites. The two approaches which significantly reduced parameter uncertainty and equifinality were: 1) the addition of the physico-chemically based DRIFTS stability index, and 2) combining several sites

https://doi.org/10.5194/bg-2019-292
Preprint. Discussion started: 7 August 2019

Biogeosciences Discussions

into one Bayesian calibration, as derived turnover rates can be strongly site specific. The combination of all four sites showed that SOM is likely lost at relatively fast turnover rates with the 95 % credibility intervals of the slow SOM pools half life ranging from 278 to 1095 years, with 426 years as a value of highest probability density. The credibility intervals of this study were consistent with several recently published Bayesian calibrations of similar SOM models, all turnover rates were considerably faster than earlier models suggested. It is therefore likely that published turnover rates understimate the potential loss of SOM.

1 Introduction

Process-based models of plant-soil ecosystems are used from plot to regional and global scales as tools of research and to support policy decisions (Campbell and Paustian, 2015). The soil organic matter (SOM) in such models is traditionally divided into several pools, representing fast, slow and for some models even inert SOM (Hansen et al., 1990; Parton et al., 1993). Common methods of SOM pool initialization assume steady state conditions or perform a model spin-up run. In the model spin-up run the user attempts to simulate the SOM dynamics according to history and carbon inputs for the decades to several millennia prior to the period of actual interest (eg. O'Leary et al., 2016). Theoretically if the SOM pools are at steady state, models can be initialized, i.e. pool sizes calculated, either by simple equations (eg. DAISY, - S. Hansen et al., 2012) or by inverse modelling (RothC - Coleman and Jenkinson, 1996). In both cases, data is insufficient to guarantee that the assumptions of SOM steady state or long-term knowledge of land use history and inputs are correct, given the lack of data of residue input and weather data for the required long-term timescales (> 200 years). Therefore, the simulation of past carbon inputs and the assumption of steady state are a rough approximation at best. It is therefore critical to find measurable proxies such as soil size density fractionation or infrared spectra, that can provide information on the quality of SOM and hence help in SOM pool initialization (Sohi et al., 2001).

As was shown by Zimmermann et al. (2007), and recently confirmed by Herbst et al. (2018), a link exists between soil fractions obtained by size and density fractionation and fast and slow cycling SOM pools. However, Poeplau et al. (2013) showed, that the same fractionation protocol led to considerably different results at six different laboratories which regularly applied the technique (coefficient of variation from 14 to 138 %). The resulting differences in the model initializations for simulated SOM loss after 40 years of fallow, lead to differences in SOM losses that were to up to 30 % of initial SOM. Hence there is a need for a reproducible proxy for SOM pool initiation.

We hypothesised that such a proxy could be obtainted from inexpensive, high-throughput Diffuse reflectance mid infrared Fourier transform spectroscopy (DRIFTS). DRIFTS can provide information on SOM quality, but also on texture and even mineralogy (Nocita et al., 2015; Tinti et al., 2015). The interaction of mid-infrared energy with molecular bonds in soil produce typical vibrational peaks of absorbance at distinct wavelengths, which can be linked to different bonds of carbon, nitogen, silicon and other elements. The vibrational peaks which relate to carbon of different complexities, such as the aliphatic C-H streching peak around 2930 cm^{-1} and the aromatic C=C streching peak at 1620 cm^{-1}, provide information on SOM quality (Giacometti et al., 2013; Margenot et al., 2015). Demyan et al. (2012) found aliphatics to be enriched under long-term farmyard manure application and depleted in mineral fertilizer or control treatments, and showed that the ratio of the 2930 cm^{-1} to 1620 cm^{-1} peaks had a significant positive correlation with the ratio of labile to stable SOM obtained by size and

https://doi.org/10.5194/bg-2019-292
Preprint. Discussion started: 7 August 2019

density fractionation. Hence, we hypothesised that the ratio of the aliphatic to aromatic DRIFTS peaks can be used as proxy for SOM pool initialization, thus providing a major improvement over assuming steady state SOM. This ratio of aliphatic to aromatic peaks, will be called DRIFTS stability index (DSI) hereafter. Testing, improvement and proper use of the DSI was the central topic of this study. Recent findings have highlighted that the residual water content in bulk soil samples after drying at different temperatures affects the DSI considerably. Water has both an absorbance reducing impact on the whole spectra and it does overshade the 2930 cm^{-1} peak (Laub et al., submitted). For this reason we also tested how the drying temperature prior DRIFTS measurements affect the use of the DSI proxy, using 32, 65 and 105°C as pretreatment temperatures.

We used the DAISY SOM model (Hansen et al., 2012) to test our hypotheses about the DSI performance. DAISY is a commonly used SOM model (Campbell and Paustian, 2015) with a typical multi-pool structure, which includes two soil microbial biomass pools, as well as two SOM pools (fast and slow). With first-order turnover kinetics and humification efficiency values (**Figure 1**Fehler! Verweisquelle konnte nicht gefunden werden.), the structure is similar to other widely used SOM models such as CENTURY (Parton et al., 1993) or ICBM (Andrén and Kätterer, 1997). In the current study only bare fallow experiments were used to avoid the complication caused by the conversion of different plant compounds into SOM of different stabilities while being recycled at several stages. A range of different sites and time scales from one to five decades were included, and the SOM pool initialization by the use of the DSI was compared to initialization by assuming steady state with different published turnover rates.

As SOM pool sizes and turnover rates are closely linked, it could also be necessary to recalibrate DAISY parameters for the use of the DSI. Therefore, a Bayesian calibration of turnover rates was done in order to adjust DAISY turnover rates to the pool division by the DSI and the change of the DSI throughout the fallow period. Thus, DAISY parameterization in respect to equifinality and uncertainty as well as dependence on model structure was evaluated. The final hypothesis was, that through a Bayesian calibration using the DSI, DAISY pools will correspond to measured, i.e. physiochemically meaningful fractions thus reducing uncertainty. The posterior credibility intervals and optima of turnover rates should correspond to the results of other Bayesian calibrations done for models with similar two-pool structures for relatively stable SOM pools. If such relations could be confirmed, this would point towards fundamental insights about the intrinsic speed of SOM turnover in temperate agroecosystems.

2 Material and Methods

2.1 Study sites and data used for modelling

We used datasets originating from bare fallow plots of four different sites with different observational durations and measurement frequencies. Samples of the 20 cm topsoil were available from the long-term experiments of (a) the Ultuna Frame trial (established in 1956, with additional data from 1979, 1995 and 2005; (Kätterer et al., 2011), four replicates), and (b) the Bad Lauchstädt Extreme Farmyard Manure Experiment (established in 1983, with additional data from 2001, 2004 and 2008, two replicates) (https://www.ufz.de/index.php?de=37008, date accessed 10.01.2019). Additional medium-term experiments (2009 until 2016) from two Southwest German regions were available of (c) the Kraichgau and (d) the Swabian Jura, representing different climatic and geological conditions. The bare fallow plots (of 5 x 5 m size) in the Southwest Germany experiments were

https://doi.org/10.5194/bg-2019-292
Preprint. Discussion started: 7 August 2019

Biogeosciences Discussions

established within agricultural fields (Ali et al., 2015) and had monthly to yearly measurement frequencies of samplings of the top 30 cm. In both regions, three replicates of bare fallow plots were established in each of three different fields. Further details on all the sites can be found in **Table 1**. All sites had been under cultivation for at least several hundred years prior to establishing the bare fallow plots.

Bulk soil samples from all experiments were analyzed for total carbon and DRIFTS spectra; samples from the Kraichgau and Swabian Jura sites were additionally analysed for soil microbial biomass carbon (SMB-C). After sampling, all bulk soil samples (except for SMB-C) were passed through a 2 mm sieve, then air dried, ball milled to powder and stored until further analysis. Their soil organic carbon (SOC) content was analyzed with a Vario Max CNS (Elementar Analysensysteme GmbH, Hanau, Germany). DRIFTS spectra of bulk soil samples were obtained (with 4 repeated measurements per sample) after 24 hr drying at 32, 65 and 105°C using an HTS-XT microplate extension, mounted to a Tensor-27 spectrometer using the processing software OPUS 7.5 (equipment and software from Bruker Optik GmbH, Ettlingen, Germany). The details: a potassium bromide (KBr) beam splitter with a nitrogen cooled HTS-XT reflection detector was used to record spectra in the mid infrared range (4000 – 400 cm^{-1}); each spectrum was a combination of 16 co-added scans with a resolution 4 cm^{-1}. Spectra were recorded in absorbance units (AU); the acquisition mode "double-sided, forward-backward" and the apodization function Blackman-Harris-3 were used. The dried samples were kept in a desiccator until measurements. After a baseline correction and a vector normalization of the spectra, peak areas were obtained as the integral on top of a local baseline with the integration limits of Demyan et al. (2012) and averaged after that. The local baselines were drawn between the intersection of the spectra and a vertical line at the integration limits (3010 – 2800 cm^{-1} for the aliphatic C-H streching, 1660 – 1580 cm^{-1} for aromatic C=C streching vibrations). Additionally, soils from the experiments in Kraichgau and Swabian Jura were analyzed for SMB-C using the chloroform fumigation extraction method (Joergensen and Mueller, 1996). Briefly, field moist samples were transported to the lab in a cooler, with extractions beginning the next day and the final SMB-C values corrected to an oven-dried (105° C) basis. The SMB-C was measured two to four times throughout the whole year. Stocks of SOC and SMB-C for the modelled layers were calculated by multiplying the percentage of SOC and SMB-C with the bulk density and depth of the modelled layer (**Table 1**). Bulk density was assumed constant for Bad Lauchstädt, Kraichgau and Swabian Jura, while for Ultuna the initial 1.44 t m^{-3} (Kirchmann et al., 2004) in the beginning was used for all but the last measurement, where 1.43 m^{-3} (Kätterer et al., 2011) was used. Due to low stone contents (< 5 %for Swabian Jura 3, < 2 % for Swabian Jura 1 and < 1 % for the other six sites), and because changes in stone content throughout the simulation periods are unlikely, no correction for stone content was done.

2.2 Description of the simulation model: DAISY Expert-N 5.0

All simulations were conducted using the DAISY SOM model (Hansen et al., 2012) integrated into the Expert-N 5.0 modelling framework. Expert-N 5.0 is a flexible modelling framework, which allows a wide range of soil, plant and water models to be combined (Heinlein et al., 2017; Klein et al., 2017; Klein, 2018). It can be compiled both for Windows and Linux systems. A detailed description of the DAISY SOM submodule as it was implemented into the Expert-N 5.0 framework can be found in Mueller et al. (1997). A graphical representation of the DAISY pools considered in this study is shown in **Figure 1**. The additional modules available for selection in the Expert-N 5.0 framework are from a range of established models for all simulated processes in the

https://doi.org/10.5194/bg-2019-292
Preprint. Discussion started: 7 August 2019

Biogeosciences
Discussions

soil-plant continuum. The evaporation, ground heat, net radiation, and emissivity were simulated according to the Penman-Monteith equation (Monteith, 1976). Water flow through the soil profile was simulated by the Hydrus-flow module (van Genuchten, 1982) with the hydraulic functions according to Mualem (1976). Heat transfer through the soil profile was simulated with the DAISY heat module (Hansen et al., 1990). In the first step of the DSI evaluation, simulations were conducted with two established parameter sets for DAISY SOM. The first set was from Mueller et al. (1997) and was a modification of the original parameter set of turnover rates in Jensen et al. (1997). The second set was established after calibrations made by Bruun et al. (2003) using the Askov Long-Term Experiments and introduced considerable changes in the turnover rates of the slow pool and the humification efficiency. An equation developed by Bruun and Jensen (2002) was used to compute the sizes of the slow and fast cycling SOM pools at steady state for both parameter sets (see next section). All the parameters of both sets are displayed in **Table 2**.

Climatic driving variables of radiation, temperature, precipitation, relative humidity and wind speed, are needed for Expert-N simulations. For the long-term experiments they were extracted from the nearest weather station with complete data (Ultuna source: Swedish Agricultural University (SLU), ECA Station ID #5506, Elevation: 15 m, Lat: 59.8100 N, Long: 17.6500 E; Bad Lauchstädt source: Deutsche Wetter Dienst (DWD) Station #2932, Elevation: 131 m, Lat: 51.4348 N, Long: 12.2396 E, Locality name: Leipzig/Halle). For the fields of the Kraichgau and Swabian Jura, the driving variables were measured by weather stations installed next to eddy covariance stations located at the center of each field. Details on the measurements, instrumentation as well as gap filling methods of eddy covariance weather stations are described by Wizemann et al. (2015).

2.3 SOM pool initializations with the DRIFTS stability index and at steady state

Measured SMB-C was divided into the slow and fast cycling microbial pools, with 10 % in the fast (8 % in Mueller et al., 1998) and 90 % in the slow pool. The remaining part of carbon (difference between total SOC and SMB-C) was divided either by the DRIFTS stability index (DSI), or according to the steady state assumption. For runs with the steady state assumption the equation of Bruun and Jensen (2002) was used, which directly computes the fraction of SOM in the slow pool at steady state from the model parameters:

$$\text{slow SOM fraction } = \frac{1}{1+\frac{k_{SOM\_slow}}{f_{SOM\_slow} * k_{SOM\_fast}}} \tag{1}$$

with k_{SOM_slow} and k_{SOM_fast} representing the turnover (per day) of the slow and fast SOM pools respectively, and f_{SOM_slow} representing the amount of fast SOM directed towards the slow SOM pool at turnover of fast SOM (humification efficiency). This resulted in 83 % of SOM being in the slow pool for the original DAISY turnover rates and 49 % in the slow pool for the Bruun et al. (2003) turnover rates (**Table 2**). For the DSI initialization, the amount of SOM in the slow pool was calculated with the formula

$$\text{slow SOM fraction} = \frac{\text{A1620cm}^{-1}}{\text{A1620cm}^{-1}+\text{A2930cm}^{-1}} \tag{2}$$

With A2930 cm^{-1} and A1620 cm^{-1} being the extracted peak areas (described in section 2.1). The remaining carbon was allocated to the fast pool. As was mentioned before, three different data inputs for the DSI were used, with drying temperatures of 32, 65 and 105°C, in order to test which drying temperature is best for modelling. An example of the change of DRIFTS spectra occurring after several years of bare fallow can be

https://doi.org/10.5194/bg-2019-292
Preprint. Discussion started: 7 August 2019

Biogeosciences Discussions

found in **Figure 2**. Each of the three DSI model initializations was then run with both published sets of parameters. Steady state initializations using **Equation 1** were only conducted with the corresponding parameter set from which they were calculated.

2.4 Statistical evaluation of model performance

Statistical analysis was performed with SAS version 9.4 (SAS Institute Inc., Cary, NC, USA). To compare different model initializations, a statistical analysis of squared model errors (SME) was conducted:

$$SME_x = (obs_x - pred_x)^2 \quad (3)$$

with obs_x being the observed value, $pred_x$ the predicted value and x the simulated variable of interest. A linear mixed model with SME_x as response was then used to test for significant differences between initialization methods. In some cases, SME_x was transformed to ensure a normal distribution of residuals (square root transformation for Ultuna SOC and Kraichgau/Swabian Jura SMB-C and forth root for Kraichgau/Swabian Jura SOC), which was checked by a visual inspection of the normal QQ plots and histograms of residuals (Kozak and Piepho, 2018). Random effects were included to account for temporal autocorrelation of SME_x within (a) the same field and (b) the same simulation. The model reads as follows:

$$y_{ijkl} = \phi_0 + \alpha_{0i} + ß_{0j} + \gamma_{0ij} + \phi_1 t_k + \alpha_{1i} t_k + ß_{1j} t_k + \gamma_{1ij} t_k + u_{kl} + u_{ijkl} \quad (4)$$

where y_{ijkl} is the SME_x of the simulation using the *i*th initialization with the *j*th parameter set, at the *k*th time on the *l*th field, ϕ_0 is an overall intercept, α_{0i} is the main effect of the *i*th initialization, $ß_{0j}$ is the main effect *j*th parameter set, γ_{0ij} is the *ij*th interaction effect of initialization x parameter set, ϕ_1 is the slope of the time variable t_k, $\alpha_{1i} t_k$ is the interaction of the *i*th initialization with time, $ß_{1j} t_k$ is the interaction of the *j*th parameter set with time, $\gamma_{1ij} t_k$ is the *ij*th interaction effect of initialization x parameter set x time, u_{kl} is the autocorrelated random deviation on the *k*th time in the *l*th field and u_{ijkl} is the autocorrelated residual error term corresponding to y_{ijkl}. The detailed SAS code can be found in the supplementary material.
For Ultuna and Bad Lauchstädt, the u_{kl} term was left out, as both trials only had one field. As the Kraichgau and Swabian Jura had the exact same experimental setup and time frame, these sites were jointly analyzed in the statistic model, but due to completely different setups and time frames, this was not possible for Bad Lauchstädt and Ultuna. The full models with all fixed effects were used to compare different correlation structures for the random effects including (i) temporal autocorrelation (exponential, spherical, Gaussian), (ii) compound symmetry (iii) a simple random effect for each different field and simulation, (iv) a random intercept and slope of the time variable (with allowed covariance between both) for each field and initialization method. A residual maximum likelihood estimation of model parameters was used and the best fitting random effect structure for this model was selected using the Akaike Information Criterion as specified by Piepho et al. (2004). Then a stepwise model reduction was conducted until only the significant effects ($p < 0.05$) remained in the final statistical model. Because a mixed model was used, the Kenward-Roger method was used for estimating the degrees of freedom (Piepho et al., 2004) and to compute post hoc Tukey-Kramer pairwise comparisons of means.

https://doi.org/10.5194/bg-2019-292
Preprint. Discussion started: 7 August 2019

Biogeosciences Discussions

2.5 Model optimization and observation weighting for Bayesian calibration

The optimization with Bayesian calibration was done for k_{SOM_slow}, k_{SOM_fast} and the humification efficiency (f_{SOM_slow}), as only those three parameters have a considerable impact on the rate of native SOM loss (we provide a detailed explanation why this is the case in the supplementary material). The Bayesian calibration method uses an iterative process to simulate what the distribution of parameters given the data and the model would be, combining a random walk through the parameter space with a probabilisitc approach on parameter selection.

The Differential Evolution Adaptive Metropolis algorithim (Vrugt, 2016) implemented in UCODE_2014 (Lu et al., 2014; Poeter et al., 2014) was used for the Bayesian calibration in this study. As no Bayesian calibration of DAISY SOM parameters has been done before, we used noninformative priors. The main drawback of noninformative priors is that they can have longer computing times, but as was shown by Lu et al. (2012) with enough data and long enough running periods, the posterior distributions are very similar to using informed priors. Ranges were set far beyond published parameters with 1.4 * 10^{-2} to 1.4 * 10^{-6} d^{-1} for k_{SOM_fast} and 1.4 * 10^{-3} to 5 * 10^{-7} d^{-1} for k_{SOM_slow}. The parameter f_{SOM_slow} had to be more strongly constrained as without constraints it tended to run into unreasonable values up to 99 % humification. The limts were therefore set to 0.05 to 0.35 for, which is +/- 5 % of the two published parameter sets and also represents the upper boundaries of other similar models (eg. Ahrens et al., 2014). As convergence criteria the default UCODE_2014 Gelman-Rubin criterion (Gelman and Rubin, 1992) with a value of 1.2 was chosen. A total of 15 chains were run in parallel with a timestep of 0.09 days in Expert-N 5.0 (this was the largest timestep and fastest computation, where the simulation results of water flow, temperature and hence SOM pools was unaltered compared to smaller timesteps). It was ensured that at least 300 runs per chain were done after the convergence criterion was satisfied.

In Bayesian calibration, a proper weighing of observations is needed in order to achieve a diagonal weight matrix of residuals (proportional to the inverse of the variance covariance matrix), and to ensure that residuals are in the same units (Poeter et al., 2005, p18 ff). This included several steps. A differencing removed autocorrelation in the individual errors in each model run of the Bayesian calibration itself (the first measurement of each kind of data at each field was taken as raw data, for any repeted measurement the difference from this first measurement was taken instead of the raw data). Details on differencing are provided in chaper 3 of the UCODE_2005 manual (Poeter et al., 2005). To account for different levels of heterogeneity of different fields in the weighting, a mixed linear model was used to separate the variance of observations from different fields originating from natural field heterogeneity from the variance originating from measurement error. To do so, a linear mixed model with random slope and intercept of the time effect for each experimental plot was fitted to the SOC, SMB-C and DSI data for each field individually:

$$y_{kl} = \phi_0 + \phi_1 t_k + u_l + u_k + u_{kl} \tag{5}$$

where y_{kl} is the modelled variable at the kth time on the lth plot, ϕ_0 is the intercept, ϕ_1 is the slope of the time variable t_k, u_l is the random intercept, u_k is the autocorrelated random deviation of the slope and u_{kl} is the autocorrelated residual error term corresponding to y_{kl}.

https://doi.org/10.5194/bg-2019-292
Preprint. Discussion started: 7 August 2019

The error variance of each type of measurement (DSI, SMC-C, SOC) at each field ${\sigma_{fM}}^2 = \sigma^2_{u_k} + \sigma^2_{u_{kl}}$ was then used for weighting of obsevations, excluding the field variance $\sigma^2_{u_l}$ from the weighting scheme. This error variance was used in UCODE_2014 to compute weighted model residuals for each observation as follows:

$$w\_SME_x = \frac{(obs_x - pred_x)^2}{\sigma^2{}_{fM}} \quad (6)$$

where *w_SME*$_x$ is the weighted squared model residual , obs_x is the observed value, $pred_x$ is the predicted value and $\sigma^2{}_{fM}$ is the error variance of the *M*th type of measuremet at each field. All w_SME_x are combined to the sum of squared weighted residuals, which is the objective function used in UCODE_2014 (Poeter et al., 2014). By this procedure, observations with higher measurement errors have a lower influence in the Bayesian calibration.

Since the medium-term experiments had a much higher measurement frequency, it was also tested if giving each experiment the same weight would improve the results of the Bayesian calibration (equal weight calibration). In this case an additional group weighting term was introduced for groups of observations, representing different datasets at the different sites. This weighting term is internally multiplied with each *w_SME*$_x$ in UCODE_2014 and was calculated as

$$w\_G_x = \frac{1}{(n_{obs} * n_{par} * n_f)} \quad (7)$$

where *w_G*$_x$ is the weight multiplier for each observation, n_{obs} is the number of observations per parameter, n_{par} is the number of parameters per field, and n_f is the number of fields per site. This weighing assures that with the exact same percentage of errors, each site would have the exact weight of 1.

The influence of several factors was assessed in this Bayesian calibration: the use of individual sites compared to combining sites, including an equal weight (as described above) vs weighting only by error variance, and the effect of in/excluding the DSI in the Bayesion calibration. Therefore, seven Bayesian calibrations were conducted in total: four for each individual site, i.e., 1) Ultuna, 2) Bad Lauchstädt, 3) Kraichgau, 4) and Swabian Jura, 5) for all sites combined with equal weighting, 6) for all sites without DSI use in the Bayesian calibration (only for initial pool partitioning) and finally 7) for all sites combined using the DSI and original weight. The comparison of these seven Bayesian calibrations was designed to assess the effect of the site on the calibration, as well as the effect of the DSI and of user weighting decisions.

3 Results

3.1 Dynamics of SOC, SMB-C and DRIFTS during bare fallows

All bare fallow plots lost SOC over time with the severity of SOC loss varying between soils and climates at the different sites. The Bad Lauchstädt site experienced the slowest carbon loss (7% of initial SOC in 26 years), while at Ultuna and Kraichgau SOC was lost at much faster rates (Ultuna - 39% of initial SOC in 50 years¸ Kraichgau on average 9% of initial SOC in 7 years) (**Table 3**). In the Swabian Jura field 1 the SOC loss was comparable to that of the Kraichgau (about 10% of initial SOC in 7 years), but was much less in fields 2 and 3. Some miscommunications with the field owner's contractors led to unwanted manure addition and fields ploughing in 2013, hence results of these two fields after the incident in 2013 were excluded. The DRIFTS spectra revealed that the aliphatic peak area (2930 cm^{-1}) decreased rather fast after the establishment of the bare

https://doi.org/10.5194/bg-2019-292
Preprint. Discussion started: 7 August 2019

fallow plot while the aromatic peak area (1620 cm^{-1}) had only minor changes and no consistent trend (**Figure 2**). The resulting amount of SOC in the slow pool according to the computed DSI changed from the initial range of 54 to 80 % to the range of 76 to 99% at the end of the observational period. The SMB-C reacted even more rapidly to the establishment of fallows and halved on average for all fields within 7 years duration.

3.2 Comparison of the different model initializations

The observed trend of SOC loss with ongoing bare fallow duration was also found in all simulations (**Figure 3**). For Ultuna, simulated SOC loss in all cases underestimated measured loss, while for Bad Lauchstädt, simulated SOC losses overestimated measured losses. At Kraichgau sites SOC loss was underestimated by the models, but using the Bruun (2003) parameter set yielded values closer to what was measured. In the Swabian Jura, both parameter sets underestimated SOC loss. The decline of SMB-C in the Kraichgau and Swabian Jura (**Figure 4**) occurred more rapidly than that of SOC, though SMB-C had higher variability of measurements. The parameter sets with steady state assumptions marked the upper and lower boundaries of the SMB-C simulations but the DRIFTS stability index (DSI) initializations were closer to the measured values (with exception of Swabian Jura field 3). For brevity only simulations of field 1 for Kraichgau and Swabian Jura are displayed here. Simulation results for fields 2 and 3 are found in the supplemental material (**Figure S 2** for SOC simulations and **Figure S 3** for SMB-C).

The statistical analysis of the model error revealed a site dependency of the effect of the parameter set. The three-way interaction of initialization, parameter set and time $\gamma_{1i}\ t_k$ was significant for all but Bad Lauchstädt SOC, where only the parameter set had a significant effect. In the case of Bad Lauchstädt, the model error was significantly lower with the slower Mueller (1997) SOM turnover parameter set, while for the rest of tested cases, the faster Bruun (2003) set performed significantly better (**Table 4**). For Ultuna and for Kraichgau + Swabian Jura SOC, the steady state assumption with Mueller (1997) had the highest model error, while the steady state assumption with Bruun (2003) had the lowest model error of all simulations, but the difference to the DRIFTS initialization using 105°C drying temperature was only significant for Ultuna and not for the other sites. For the SMB-C simulations in the Kraichgau + Swabian Jura, however, the errors were lowest for the DRIFTS initialization using the 105° C drying temperature with Bruun (2003) parameters and significantly lower than both steady state initializations. Of the DRIFTS initializations using different drying temperatures, the model error was always lowest when using the 105°C drying temperature initialization compared to 32°C and 65°C (significant for Ultuna, as well as for Kraichgau + Swabian Jura SMB-C using Mueller (1997) parameters). As initializations with DRIFTS using 105°C drying temperature consistently performed the best of all three DRIFTS initializations, it was chosen to continue only with DRIFTS spectra of soils dried at 105°C for the Bayesian calibration.

3.3 Informed turnover rates of the Bayesian calibration

The posterior distribution of parameters from the Bayesian calibration differed considerably between the different calibrations for individual sites, but there were also differences between different weighting schemes and to the Bayesian calibration without DSI when using all sites (**Figure 5**). The highest probability turnover of the fast SOM pool (k_{SOM_fast}) was 1.5 and 3 times faster for Ultuna and Kraichgau respectively, when compared to initial rates (1.4 * 10^{-4} d^{-1} for both parameters sets), which fitted well for Bad Lauchstädt and Swabian Jura. For the slow SOM pools (k_{SOM_slow}) the Bad Lauchstädt, Kraichgau and Swabian Jura site calibrations were in between the two published parameter sets, but tended towards the slower rates ($2.7 * 10^{-6}$ d^{-1} by Mueller (1997)), while the optimum for Ultuna was exactly at the fast rates of Bruun (2003) ($4.3 * 10^{-5}$ d^{-1}). The humification efficiency (f_{SOM_slow}) was not strongly constrained in the Bayesian calibration, except for the Kraichgau site, where it ran into the upper boundary of 0.35. This trend towards higher humification existed also for the other sites, but with much less strength than for Kraichgau.

The different calibrations of the combination of all sites under different weightings and with or without the DSI also led to considarable differences in the posteriors. When combining the sites with the artificial equal weighting, the posterior distribution of all three parameters was the widest, basically covering the range of all four sites calibrations. With the original weighting scheme, only informed by the variance of the data, the posteriors were much more narrow for all parameters with the optima of k_{SOM_fast} being slightly faster than the two (similar) published rates. The optima of k_{SOM_slow} were slightly slower than that of Bruun (2003) but much faster than that of Mueller (1997) and f_{SOM_slow} was even above the higher value of 0.3 by Bruun (2003). The use of the original weighting scheme but without the use of the DSI in the Bayesian calibration did not constrain the f_{SOM_slow} at all and had faster k_{SOM_slow} and slower k_{SOM_fast} than the one using the DSI. Both these Bayesian calibrations using the original weighting (with and without DSI) showed a trend towards slightly faster turnover than was suggested by Bruun (2003).

There was a strong negative correlation between k_{SOM_fast} and k_{SOM_slow} parameters for all but the Bad Lauchstädt calibration (**Figure S 4**). When DSI was not included, this negative correlation was stronger than when it was included in the Bayesian calibration (**Figure 6**). The parameters k_{SOM_fast} and f_{SOM_slow} were always correlated positively, most strongly for Kraichgau (0.49) and Swabian Jura (0.38), but only weakly for the long-term sites. The correlations between the parameters k_{SOM_slow} and f_{SOM_slow} were generally low and both positive and negative. The parameters with the highest probability density of the calibrations combining all sites for f_{SOM_slow} , k_{SOM_fast} and k_{SOM_slow} in that order were 0.34, $2.29 * 10^{-4}$, $3.25 * 10^{-5}$ for the original weight calibration and 0.06, $9.58 * 10^{-5}$ and $5.54 * 10^{-5}$ for the calibration using original weights and no DSI, showing that turnover rates of k_{SOM_slow} of very similar magnitude as k_{SOM_fast} were possible without the use of the DSI. About 10 % of simulations of the Bayesian calibration without DSI had even a faster k_{SOM_slow} *than* k_{SOM_fast}.

4 Discussion

4.1 How useful is the DRIFTS stability index?

The results of this study confirm the hypothesized usefulness of the DRIFTS stability index for SOM pool partitioning for a number of soils across Europe. The DSI therefore is a proxy of the current state of SOM in a particular field. This is particularly relevant, given that the changes in genotypes of crops, agricultural management, crop rotations and the rise of average temperatures in recent decades probably have affected the past quality and quantity of carbon inputs to soil. Consequently, the steady state assumption for model initialization is not likely to be valid. A search for suitable proxies for SOM pool partitioning into SOM model pools that correspond to measurable and physiochemically meaningful quantities is therefore of high interest (Abramoff et al., 2018; Bailey et al., 2018; Segoli et al., 2013). Despite the acknowledged mineral interference of the DSI, Demyan et al. (2012) showed that with a careful selection of integration limits, the DSI is a sensitive indicator of SOM stability if mineralogy is similar. With the results from our study we could not reject the

https://doi.org/10.5194/bg-2019-292
Preprint. Discussion started: 7 August 2019

Biogeosciences
Discussions

hypothesized usefulness of the DSI for SOM pool partitioning for soils of different properties across Europe. The statistical analysis of the model error showed clearly that the DSI does improve poor model performance, especially with the slower turnover rates of Mueller (1997). When model performance is already satisfactory, the natural variability of the DSI can make model performance worse, as in the case of Ultuna SOC with Bruun (2003) parameters, but this reduction was minor compared to the improvement the DSI had over steady state assumptions at Ultuna with Mueller (1997) rates. The better results for Ultuna with the Bruun (2003) steady state might also just be an effect of turnover times still being too slow and hence the more SOC in the fast pool, the faster the general turnover. This was also indicated by faster optima by the Bayesian calibration compared to both published turnover rates. Also in the case of Bad Lauchstädt, turnover rates had a high influence on model performance. The properties of a Chernozem were generally not well captured with both parameter sets, and it has probably a slower SOM decomposition as many other agricultural soils. Nevertheless, the use of DSI also was suitable for Bad Lauchstädt, as it did also not reduce model performance.

The results for SMB-C, typically the pool that reacts fastest to changes of input, corroborated the evidence that the DSI initialization is a more realistic estimation of SOM pools than the steady state assumption. The range of different sites, soils, and climatic conditions of Europe represented within this study suggest robustness of the DSI proxy for SOM quality and SOM pool division for a large environmental gradient. Hence it would be an improvement over assuming steady state of SOM wherever there is a lack of detailed information of carbon inputs and climatic conditions. Considering the timescales at which SOM develops, this is almost anywhere, as detailed data is available at best for <200 years, which is not even one half-life of the slow SOM pool.

So far, studies that assessed SOM quality and pool division proxies, either using thermal stability of SOM (Cécillon et al., 2018) or size-density fractionation (Zimmermann et al., 2007), only indirectly related the proxies to inversely modelled SOM pool distributions, using machine learning and rank correlations. In contrast, our study showed that the DSI is a proxy which can be directly used for pool initialization. As for other proxies such as thermal stability (Demyan et al., 2013) and size density fractionation (Puttaso et al., 2013), the relationship between SOM quality and the DSI is only indirect as e.g. determined by comparing high/low SOM treatments in manipulation experiments. However, the DSI also makes sense from the perspective of energy content of the molecules that create the peaks of absorption, as microorganisms can obtain more energy from the breakdown of aliphatics are compared to aromatics (e.g. Good and Smith, 1969), and therefore aliphatics are primarily targeted by microorganisms (hence have faster turnover) as previously shown for bare fallows (Barré et al., 2016).

The two distinct peaks for aliphatic and aromatic carbon bonds of the DSI fit well to the two SOM pool structure of DAISY and the simulation of carbon flow through the soil in DAISY is very similar to several established SOM models such as SoilN, ICBM and CENTURY. It is therefore likely that with calibration, the DSI could be used as a general proxy for SOM models with two SOM pools and a humification efficiency (f_{SOM_slow} in DAISY). The parameter correlations between k_{SOM_slow}, k_{SOM_fast} and f_{SOM_slow} according to the Bayesian calibrations also showed clearly that, as Bruun and Jensen (2002) postulated, the three parameters are strongly related, and without the DSI modifying anyone of them can lead to the same results in terms of SOC and SMB-C simulation. Without the DSI, no clear distinction between fast and slow pools in the calibration was given as can be seen by sometimes faster k_{SOM_slow} than k_{SOM_fast}. Assigning the DSI to DAISY not only reduced the correlations, but also made this clear distinction between fast and slow pool in the Bayesian calibration.

https://doi.org/10.5194/bg-2019-292
Preprint. Discussion started: 7 August 2019

The aliphatic carbon peak of DRIFTS is most resolved when applying a 105°C drying temperature (Laub et al., submitted). The results from modelling corroborated the finding that the DSI should be obtained from measurements after drying at 105 °C with the performance of the DRIFTS initializations being always in the order 105°C > 65°C > 32°C drying temperature (differences being sometimes but not always significant).

Compared with the other proxies for SOM quality discussed above, the measurements by DRIFTS are inexpensive, relatively simple, and the equipment of the same manufacturer is standardized. This should also constrain variability between different laboratories and be attractive for large-scale applications with large sample size, for example to initialize simulations at the regional scale. The recent coupling of pyrolysis with DRIFTS (Nkwain et al., 2018) might be a further advancement of the DSI, as it overcomes mineral interferences in the spectra. However, this technique is more complex due to a larger number of visible organic peaks, including CO_2 that develops from the pyrolysis, which makes it not easily applicable to established two-pool models such as DAISY. In addition, a considerable portion (30 – 40 %) of SOM is not pyrolyzed and therefore not recorded in the spectra. In summary, it was found that the DSI can be directly used to distribute SOM between pools in two pool models, though there is some mineral interference. Furthermore, DSI was suitable for a wide range of soils and improved model performance. Hence, DSI seems to be a more robust proxy for pool initialization then methods such as steady state or long-term spin-up runs which rely on strong assumptions to which they are very sensitive though there is very limited data to prove them.

4.2 Parameter uncertainty as estimated with Bayesian calibration

According to our Bayesian calibrations, a wide range of parameter values are possible for DAISY going far beyond the initial published parameter sets. By combining various sites and including meaningful proxies, such as the DSI, the parameter uncertainty and equifinality could be reduced and the credibility intervals narrowed. The predictions of mechanistic models usually fail to account for the three main statistical uncertainties of (1) inputs, (2) scientific judgments resulting in different model setups and (3) driving data (Wattenbach et al., 2006). However, with a Bayesian calibration framework such as implemented in UCODE 2014, almost any model can be made probabilistic. Then the uncertainties of parameters and outputs can be assessed, even for projections into the future (Clifford et al., 2014). As this study focused on Bayesian calibration and we used an established model, we address mainly the parameter uncertainty, although input uncertainty was also included through the weighting process. We clearly demonstrated an effect of the individual site used for Bayesian calibration on the resulting model parameters and uncertainties. Similarly diverging site specific turnover rates were also found by Ahrens et al. (2014) in a study of soil carbon in forests. Diverging results for different sites generally point towards a need for a better understanding of the modelled system and model improvements (Poeter et al., 2005), but this often requires a deeper understanding of the system and new measurements – hence it is not always feasible. A Bayesian calibration asks the question: "What would be the probability distribution of parameters, given that the measured data should be represented by the selected model?". Hence, if only one site is used, it can only answer this question for that specific site. As this study showed, the parameter set could then be highly biased for other sites. For a more robust calibration, several sites should be combined to obtain posterior distributions of parameters for a gradient of sites, though this might reduce model performance for individual sites. The introduction of the equal weighting scheme, which gave similar weights to the different sites, highlights how much bias may be introduced by user decisions of artificial weighting: this Bayesian calibration

https://doi.org/10.5194/bg-2019-292
Preprint. Discussion started: 7 August 2019

parameter set had the highest uncertainties and it appears as if the Ultuna site had by far the strongest influence. In contrast to that, the combination of all four sites with the original weights based on the error variances or measurements led to a very clear reduction of parameter uncertainty and the narrowest parameter credibility intervals (**Figure 6 a** compared to **b** and **c**).

The results of the statistical analysis of model errors (**Table 4**) suggests that the DSI is suitable for pool initialization. This was corroborated by the Bayesian calibration, as the inclusion of the DSI narrowed credibility intervals for the slow SOM pool turnover and humification efficiency and reduced the correlation between fast and slow SOM turnover compared to the simulation without the DSI as constraint. Especially the clear distinction between k_{SOM_slow} and k_{SOM_fast} shows the advantage of attaching a physiochemical meaning to the pools that was not given before. Finding new and meaningful proxies is therefore crucial in addressing the equifinality originating from the complex model structures and hence to reduce model uncertainty. While we demonstrated this with the DSI, it is a general principle which others have used in similarly effective approaches, for example within a time series of ^{14}C data (Ahrens et al., 2014) and the combination of several meaningful proxies would likely lead to the best results.

Of all three parameters, the humification efficiency (f_{SOM_slow}) was the only parameter that consistently ran into the upper boundaries, set to 35 %. In fact, initial calibrations were done where f_{SOM_slow} was constrained to 95 %; even then, it tended to run into that constraint (**Figure S 5**) and led to much faster turnover rates (k_{SOM_slow}) than were published before. These high values of f_{SOM_slow} were so far above the published 10 % for the Mueller (1997) dataset and 30 % for Bruun (2003) but also any other published model, that this was considered a model formulation problem, which did not depend on whether the DSI was included in the Bayesian calibration or not. Only when the humification efficiency was restricted in the Bayesian calibration, the turnover of fast and slow SOM aligned with the earlier published rates.

4.3 Model structure determines SOM turnover times in two-pool models

The rate of SOM decomposition remains of major interest, especially with respect to the potential of SOM as a global carbon sink (Minasny et al., 2017). First conceptual approaches proposed residence times of 1000 years and longer (e.g. in CENTURY, Parton et al., 1987), but the SOM models were calibrated to fit data measured in long-term experiments that included vegetation. The pool structure of early SOM models such as DAISY and CENTURY were rather similar as were the turnover rates of SOM pools (see summary in **Table 5**). An improved understanding of actual amounts of carbon inputs to the soil, which still remain challenging to measure, led to faster turnover rates in more recent model versions (e.g. by Bruun, 2003). The reason is probably that inputs of carbon and nitrogen to the soil were often underestimated as it is very difficult to measure root turnover and rhizosphere exudation inputs without expensive in situ ^{13}C or ^{14}C labeling. The underestimated inputs were then likely counterbalanced in the model calibration by slower turnover rates resulting in acceptable model outputs (SOM dynamics and CO_2 emissions) for the time being. However, as our summary of more recent studies underlines (**Table 5**), the earlier published turnover rates seem to be subject a systematic underestimation. As the comparison of our Bayesian calibration to other recent Bayesian calibration studies suggest, the relatively fast turnover rates of this study are in alignment with other recent findings (**Table 5**), as all five examples have published turnover rates for the slow SOM pool, which are at least one order of magnitude faster than early assumptions from the 1980s and 90s.

https://doi.org/10.5194/bg-2019-292
Preprint. Discussion started: 7 August 2019

Biogeosciences
Discussions
Open Access

This also shows how critical it is to understand model uncertainties and to test fundamental assumptions of how SOM is transferred between the pools (Sulman et al., 2018). The comparison between constrained and unconstrained humification efficiency in the Bayesian calibrations suggest that the sequential flow of carbon through the system might be assuming a condensation of stabile carbon that does not actually explain the vast majority of slow SOM formation.

From a theoretical perspective, one may wonder how large amounts of less complex SOM should become complex SOM without any involvement of living soil organisms. The way that the formation of complex carbon is represented in DAISY is probably a remainder of earlier humification theories from the 1990s that mostly ignored microbe involvement, while most of the recent studies suggest that the vast majority of SOM is of microbial origin (Cotrufo et al., 2013). A simple adaption for two-pool SOM models such as DAISY that include SMB pools could acknowledge this paradigm shift: The partitioning between slow and fast turnover SOM could be at the death of the microbial biomass (**Figure 7**) without any transfer of SOM from fast to slow pools. This would also be in alignment with the DSI concept, as aliphatic carbon should not spontaneously transform to aromatic carbon on its own. Then DAISY would fit better to the DSI and other proxies linking measurable fractions to SOM pools (the same is true for CENTURY and other models, which apply the same humification principle). The way that pools are linked in the current setup, the actual turnover time of recalcitrant SOM consists of the turnover of the fast pool and the slow pool combined as it moves through these pools sequentially (**Figure 1**Fehler! Verweisquelle konnte nicht gefunden werden.).

How strongly the basic assumptions influence SOM simulation is also reflected when differences between one- and two-SOM pool models are compared. The turnover rates of the one-pool models are in between those of slow and fast pools. However, our comparison shows that models with similar structure come to similar conclusions for SOM turnover. For example, the one-pool model in Clifford et al. (2014) was quite similar in turnover rates to that in Luo et al. (2016), but does not match well with two-pool models. Then again the rates for the two-pool models of this study, and the studies by Ahrens et al. (2014) and Hararuk et al. (2017) were very similar in their minima and maxima, for both the slow and fast SOM pools, which shows that only models with a similar number of pools and transformations could be compared.

The 95 % credibility intervals of half-lives in DAISY in the range from 278 to 1095 years for the slow pool and from 47 to 90 years for the fast pool for the combination of sites presented here. If these values were reasonable – and as the three recent Bayesian calibrations including this study are quite close in turnover rates (**Table 5**), this seems to be the case, SOM could be lost at much faster rates under mismanagement and global warming than earlier modeling results suggest. The rates still also be biased towards an underestimation of turnover, as even with intense efforts it is next to impossible to keep bare fallow plots completely free of vegetation (weeds) and roots from neighboring plots. Recent studies are in alignment with the possibility of relatively fast SOC loss across various scales from field scale (Poyda et al., 2019) to country scale, for example in Germany, agricultural soils are much more often a carbon source than a sink (Jacobs et al., 2018). This highlights the importance of proper SOM management and a deeper understanding of the processes at different scales. Especially in the context of understanding the response of SOM to climate change it is not enough if the SOM balance is simulated appropriately, but also fluxes within the plant-soil system need to be quantified. The reason is that under a warmer climate and dryer soils, the plant-derived carbon inputs will change. Furthermore, soil enzymatic

https://doi.org/10.5194/bg-2019-292
Preprint. Discussion started: 7 August 2019

analysis at regional and field level (Ali et al., 2015, 2018) suggest that pools of different complexity have different temperature sensitivities (Lefèvre et al., 2014), which is also realized in new models (Hararuk et al., 2017). If the different pools would have different responses to temperature, the formula by Bruun and Jensen (2002) for SOM pool distribution could not be used anymore, as it implicitly assumes a similar temperature sensitivity for all pools. In the light of this, new proxies such as the DSI, soil fractionation or ^{14}C use (Menichetti et al., 2016), which could also be combined, are crucial for making SOM pools chemically or physically meaningful and to reduce model uncertainty and equifinality. A better understanding and the use of meaningful proxies such as DRIFTS, pyrolysis with DRIFTS (Nkwain et al., 2018) or thermal deconvolution (Cécillon et al., 2018; Demyan et al., 2013) in combination with Bayesian calibration and a wide range of long-term experiments are needed. The discrepancy between simulating SOM of tropical and temperate soils, which still points towards a lack of understanding of fundamental difference in processes at work on the global scale would be the best test for future proxies and SOM models, which should be facilitated by freely available datasets for model testing and calibration.

5 Conclusion

We tested the use of the DRIFTS stability index as a proxy for initializing the two SOM pools in the DAISY model and used a Bayesian calibration to implement this proxy. A statistical analysis of model errors suggested that the DRIFTS stability index initialization significantly reduced model errors in most cases, especially with initially poor performance. It therefore seems to be a robust proxy to distinguish between fast and slow cycling SOM in order to initialize two-pool models, and also adds physiochemical meaning to the pools. As also other studies show, statistically sound approaches such as Bayesian calibration are needed to grasp the high uncertainty of SOM turnover, which is often neglected in modelling exercises. Meaningful proxies such as DRIFTS, physical/chemical fractionation or ^{14}C are likely to be the most robust way to initialize SOM pools. The results of this study suggest that the turnover of SOM could be much faster than assumed by most commonly used SOM models. For example, the 95 % credibility intervals of the slow SOM pool half-live of this study ranged from 278 to 1095 years. The variability of parameters highlights the importance to include meaningful proxies into SOM models and to conduct research on a larger gradient of soils with bare fallow and planted sites, and over longer time frames.

6 Acknowledgements

This work and manuscript were supported by the German Research Foundation (DFG) under the project FOR1695 "Agricultural Landscapes under Global Climate Change – Processes and Feedbacks on a Regional Scale" within subproject P3 (CA 598/6-1). We would like to thank Elke Schulz from the Department of Soil Ecology, Helmholtz Centre for Environmental Research in Halle/Saale for the provision of samples from Bad Lauchstädt. We would also like to thank Steffen Mehl, from the UCODE development team, for his help with the weighing of observations and the troubleshooting during the setup of UCODE_2014 on the bWUniCluster. The authors acknowledge support by the state of Baden-Württemberg through bwHPC.

7 Data availability

Data of SOC from Ultuna and Bad Lauchstädt has already been published in the last decades and is cited in the text. The data of Kraichgau and Swabian Jura has not been published yet, but is provided in the graphs. All measurements of DRIFTS are unpublished to this point. We are happy to make the full dataset publicly available, once accepted for publication.

8 References

Abramoff, R., Xu, X., Hartman, M., O'Brien, S., Feng, W., Davidson, E., Finzi, A., Moorhead, D., Schimel, J., Torn, M. and Mayes, M. A.: The Millennial model: in search of measurable pools and transformations for modeling soil carbon in the new century, Biogeochemistry, 137(1–2), 51–71, doi:10.1007/s10533-017-0409-7, 2018.

Ahrens, B., Reichstein, M., Borken, W., Muhr, J., Trumbore, S. E. and Wutzler, T.: Bayesian calibration of a soil organic carbon model using $\Delta^{14}C$ measurements of soil organic carbon and heterotrophic respiration as joint constraints, Biogeosciences, 11(8), 2147–2168, doi:10.5194/bg-11-2147-2014, 2014.

Ali, R. S., Ingwersen, J., Demyan, M. S., Funkuin, Y. N., Wizemann, H.-D., Kandeler, E. and Poll, C.: Modelling in situ activities of enzymes as a tool to explain seasonal variation of soil respiration from agro-ecosystems, Soil Biol. Biochem., 81, 291–303, doi:10.1016/j.soilbio.2014.12.001, 2015.

Ali, R. S., Kandeler, E., Marhan, S., Demyan, M. S., Ingwersen, J., Mirzaeitalarposhti, R., Rasche, F., Cadisch, G. and Poll, C.: Controls on microbially regulated soil organic carbon decomposition at the regional scale, Soil Biol. Biochem., 118(December 2017), 59–68, doi:10.1016/j.soilbio.2017.12.007, 2018.

Andrén, O. and Kätterer, T.: ICBM: The introductory carbon balance model for exploration of soil carbon balances, Ecol. Appl., 7(4), 1226–1236, doi:10.1890/1051-0761(1997)007[1226:ITICBM]2.0.CO;2, 1997.

Bailey, V. L., Bond-Lamberty, B., DeAngelis, K., Grandy, A. S., Hawkes, C. V., Heckman, K., Lajtha, K., Phillips, R. P., Sulman, B. N., Todd-Brown, K. E. O. and Wallenstein, M. D.: Soil carbon cycling proxies: Understanding their critical role in predicting climate change feedbacks, Glob. Chang. Biol., 24(3), 895–905, doi:10.1111/gcb.13926, 2018.

Barré, P., Plante, A. F., Cécillon, L., Lutfalla, S., Baudin, F., Bernard, S., Christensen, B. T., Eglin, T., Fernandez, J. M., Houot, S., Kätterer, T., Le Guillou, C., Macdonald, A., van Oort, F. and Chenu, C.: The energetic and chemical signatures of persistent soil organic matter, Biogeochemistry, 130(1–2), 1–12, doi:10.1007/s10533-016-0246-0, 2016.

Bruun, S. and Jensen, L. S.: Initialisation of the soil organic matter pools of the Daisy model, Ecol. Modell., 153(3), 291–295, doi:10.17665/1676-4285.20155108, 2002.

Bruun, S., Christensen, B. T., Hansen, E. M., Magid, J. and Jensen, L. S.: Calibration and validation of the soil organic matter dynamics of the Daisy model with data from the Askov long-term experiments, Soil Biol. Biochem., 35(1), 67–76, doi:10.1016/S0038-0717(02)00237-7, 2003.

Campbell, E. E. E. and Paustian, K.: Current developments in soil organic matter modeling and the expansion of model applications: a review, Environ. Res. Lett., 10(12), 123004, doi:10.1088/1748-9326/10/12/123004, 2015.

Cécillon, L., Baudin, F., Chenu, C., Houot, S., Jolivet, R., Kätterer, T., Lutfalla, S., Macdonald, A., van Oort, F., Plante, A. F., Savignac, F., Soucémarianadin, L. N. and Barré, P.: A model based on Rock-Eval thermal analysis to quantify the size of the centennially persistent organic carbon pool in temperate soils, Biogeosciences, 15(9), 2835–2849, doi:10.5194/bg-15-2835-2018, 2018.

Clifford, D., Pagendam, D., Baldock, J., Cressie, N., Farquharson, R., Farrell, M., Macdonald, L. and Murray, L.: Rethinking soil carbon modelling: a stochastic approach to quantify uncertainties, Environmetrics, 25(4), 265–278, doi:10.1002/env.2271, 2014.

Coleman, K. and Jenkinson, D. S.: RothC-26.3 - A Model for the turnover of carbon in soil, in Evaluation of Soil Organic Matter Models, pp. 237–246, Springer Berlin Heidelberg, Berlin, Heidelberg., 1996.

Cotrufo, M. F., Wallenstein, M. D., Boot, C. M., Denef, K. and Paul, E.: The Microbial Efficiency-Matrix Stabilization (MEMS) framework integrates plant litter decomposition with soil organic matter stabilization: do labile plant inputs form stable soil organic matter?, Glob. Chang. Biol., 19(4), 988–995, doi:10.1111/gcb.12113, 2013.

Demyan, M. S., Rasche, F., Schulz, E., Breulmann, M., Müller, T. and Cadisch, G.: Use of specific peaks obtained by diffuse reflectance Fourier transform mid-infrared spectroscopy to study the composition of organic matter in a Haplic Chernozem, Eur. J. Soil Sci., 63(2), 189–199, doi:10.1111/j.1365-2389.2011.01420.x, 2012.

Demyan, M. S., Rasche, F., Schütt, M., Smirnova, N., Schulz, E. and Cadisch, G.: Combining a coupled FTIR-EGA system and in situ DRIFTS for studying soil organic matter in arable soils, Biogeosciences, 10(5), 2897–2913, doi:10.5194/bg-10-2897-2013, 2013.

Gelman, A. and Rubin, D. B.: Inference from Iterative Simulation Using Multiple Sequences, Stat. Sci., 7(4), 457–472, doi:10.1214/ss/1177011136, 1992.

van Genuchten, M. T.: A comparison of numerical solutions of the one-dimensional unsaturated—saturated flow and mass transport equations, Adv. Water Resour., 5(1), 47–55, doi:10.1016/0309-1708(82)90028-8, 1982.

Giacometti, C., Demyan, M. S., Cavani, L., Marzadori, C., Ciavatta, C. and Kandeler, E.: Chemical and microbiological soil quality indicators and their potential to differentiate fertilization regimes in temperate agroecosystems, Appl. Soil Ecol., 64, 32–48, doi:10.1016/j.apsoil.2012.10.002, 2013.

Good, W. D. and Smith, N. K.: Enthalpies of combustion of toluene, benzene, cyclohexane, cyclohexene, methylcyclopentane, 1-methylcyclopentene, and n-hexane, J. Chem. Eng. Data, 14(1), 102–106, doi:10.1021/je60040a036, 1969.

Hansen, S., Jensen, L. S., Nielsen, N. E. and Svendsen, H.: DAISY - Soil Plant Atmosphere System Model., Copenhagen: The Royal Veterinary and Agricultural University., 1990.

Hararuk, O., Shaw, C. and Kurz, W. A.: Constraining the organic matter decay parameters in the CBM-CFS3 using Canadian National Forest Inventory data and a Bayesian inversion technique, Ecol. Modell., 364, 1–12, doi:10.1016/j.ecolmodel.2017.09.008, 2017.

Heinlein, F., Biernath, C., Klein, C., Thieme, C. and Priesack, E.: Evaluation of Simulated Transpiration from Maize Plants on Lysimeters, Vadose Zo. J., 16(1), 0, doi:10.2136/vzj2016.05.0042, 2017.

Herbst, M., Welp, G., Macdonald, A., Jate, M., Hädicke, A., Scherer, H., Gaiser, T., Herrmann, F., Amelung, W. and Vanderborght, J.: Correspondence of measured soil carbon fractions and RothC pools for equilibrium and non-equilibrium states, Geoderma, 314(November 2017), 37–46, doi:10.1016/j.geoderma.2017.10.047, 2018.

Jacobs, A., Flessa, H., Don, A., Heidkamp, A., Prietz, R., Dechow, R., Gensior, A., Poeplau, C., Riggers, C., Schneider, F., Tiemeyer, B., Vos, C., Wittnebel, M., Müller, T., Säurich, A., Fahrion-Nitschke, A., Gebbert, S., Hopfstock, R., Jaconi, A., Kolata, H., Lorbeer, M., Schröder, J., Laggner, A., Weiser, C. and Freibauer, A.: Landwirtschaftlich genutzte Böden in Deutschland – Ergebnisse der Bodenzustandserhebung - Thünen Report 64, Johann Heinrich von Thünen-Institut, Bundesallee 50, 38116 Braunschweig, Germany., 2018.

Jensen, L. S., Mueller, T., Nielsen, N. E., Hansen, S., Crocker, G. J., Grace, P. R., Klír, J., Körschens, M. and Poulton, P. R.: Simulating trends in soil organic carbon in long-term experiments using the soil-plant-atmosphere model DAISY, Geoderma, 81(1), 5–28, doi:http://dx.doi.org/10.1016/S0016-7061(97)88181-5, 1997.

Joergensen, R. G. and Mueller, T.: The fumigation-extraction method to estimate soil microbial biomass: Calibration of the kEC value, Soil Biol. Biochem., 28(1), 25–31, doi:10.1016/0038-0717(95)00102-6, 1996.

Kätterer, T., Bolinder, M. A., Andrén, O., Kirchmann, H. and Menichetti, L.: Roots contribute more to refractory soil organic matter than above-ground crop residues, as revealed by a long-term field experiment, Agric. Ecosyst. Environ., 141(1–2), 184–192, doi:10.1016/j.agee.2011.02.029, 2011.

https://doi.org/10.5194/bg-2019-292
Preprint. Discussion started: 7 August 2019

Kirchmann, H., Haberhauer, G., Kandeler, E., Sessitsch, A. and Gerzabek, M. H.: Effects of level and quality of organic matter input on carbon storage and biological activity in soil: Synthesis of a long-term experiment, Global Biogeochem. Cycles, 18(4), n/a-n/a, doi:10.1029/2003GB002204, 2004.

Klein, C., Biernath, C., Heinlein, F., Thieme, C., Gilgen, A. K., Zeeman, M. and Priesack, E.: Vegetation Growth Models Improve Surface Layer Flux Simulations of a Temperate Grassland, Vadose Zo. J., 16(13), 0, doi:10.2136/vzj2017.03.0052, 2017.

Klein, C. G.: Modeling fluxes of energy and water between land surface and atmosphere for grass- and cropland system, Fakultät Wissenschaftszentrum Weihenstephan., 2018.

Kozak, M. and Piepho, H. P.: What's normal anyway? Residual plots are more telling than significance tests when checking ANOVA assumptions, J. Agron. Crop Sci., 204(1), 86–98, doi:10.1111/jac.12220, 2018.

Laub, M., Blagodatsky, S., Funkuin, Y. N. and Cadisch, G.: Soil sample drying temperature affects specific organic mid-DRIFTS peaks and quality indices, Submitt. - Geoderma, n.d.

Lefèvre, R., Barré, P., Moyano, F. E., Christensen, B. T., Bardoux, G., Eglin, T., Girardin, C., Houot, S., Kätterer, T., van Oort, F. and Chenu, C.: Higher temperature sensitivity for stable than for labile soil organic carbon - Evidence from incubations of long-term bare fallow soils, Glob. Chang. Biol., 20(2), 633–640, doi:10.1111/gcb.12402, 2014.

Lu, D., Ye, M. and Hill, M. C.: Analysis of regression confidence intervals and Bayesian credible intervals for uncertainty quantification, Water Resour. Res., 48(9), 1–20, doi:10.1029/2011WR011289, 2012.

Lu, D., Ye, M., Hill, M. C., Poeter, E. P. and Curtis, G. P.: A computer program for uncertainty analysis integrating regression and Bayesian methods, Environ. Model. Softw., 60(October), 45–56, doi:10.1016/j.envsoft.2014.06.002, 2014.

Luo, Z., Wang, E., Shao, Q., Conyers, M. K. and Liu, D. L.: Confidence in soil carbon predictions undermined by the uncertainties in observations and model parameterisation, Environ. Model. Softw., 80, 26–32, doi:10.1016/j.envsoft.2016.02.013, 2016.

Margenot, A. J., Calderón, F. J., Bowles, T. M., Parikh, S. J. and Jackson, L. E.: Soil Organic Matter Functional Group Composition in Relation to Organic Carbon, Nitrogen, and Phosphorus Fractions in Organically Managed Tomato Fields, Soil Sci. Soc. Am. J., 79(3), 772, doi:10.2136/sssaj2015.02.0070, 2015.

Menichetti, L., Kätterer, T. and Leifeld, J.: Parametrization consequences of constraining soil organic matter models by total carbon and radiocarbon using long-term field data, Biogeosciences, 13(10), 3003–3019, doi:10.5194/bg-13-3003-2016, 2016.

Minasny, B., Malone, B. P., McBratney, A. B., Angers, D. A., Arrouays, D., Chambers, A., Chaplot, V., Chen, Z.-S., Cheng, K., Das, B. S., Field, D. J., Gimona, A., Hedley, C. B., Hong, S. Y., Mandal, B., Marchant, B. P., Martin, M., McConkey, B. G., Mulder, V. L., O'Rourke, S., Richer-de-Forges, A. C., Odeh, I., Padarian, J., Paustian, K., Pan, G., Poggio, L., Savin, I., Stolbovoy, V., Stockmann, U., Sulaeman, Y., Tsui, C.-C., Vågen, T.-G., van Wesemael, B. and Winowiecki, L.: Soil carbon 4 per mille, Geoderma, 292, 59–86, doi:10.1016/j.geoderma.2017.01.002, 2017.

Monteith, J. L.: Evaporation and surface temperature, Q. J. R. Meteorol. Soc., 12, 513–522, doi:10.1002/qj.49710745102, 1976.

Mualem, Y.: A new model for predicting the hydraulic conductivity of unsaturated porous media, Water Resour. Res., 12(3), 513–522, doi:10.1029/WR012i003p00513, 1976.

Mueller, T., Jensen, L. S. S., Magid, J. and Nielsen, N. E. E.: Temporal variation of C and N turnover in soil after oilseed rape straw incorporation in the field: simulations with the soil-plant-atmosphere model DAISY, Ecol. Modell., 99(2), 247–262, doi:http://dx.doi.org/10.1016/S0304-3800(97)01959-5, 1997.

Mueller, T., Magid, J., Jensen, L. S., Svendsen, H. and Nielsen, N. E.: Soil C and N turnover after incorporation of chopped maize, barley straw and blue grass in the field: Evaluation of the DAISY soil–organic-matter submodel, Ecol. Modell., 111(1), 1–15, doi:10.1016/S0304-3800(98)00094-5, 1998.

Nkwain, F. N., Demyan, M. S., Rasche, F., Dignac, M.-F., Schulz, E., Kätterer, T., Müller, T. and Cadisch, G.:

Coupling pyrolysis with mid-infrared spectroscopy (Py-MIRS) to fingerprint soil organic matter bulk chemistry, J. Anal. Appl. Pyrolysis, 133(April 2017), 176–184, doi:10.1016/j.jaap.2018.04.004, 2018.

Nocita, M., Stevens, A., van Wesemael, B., Aitkenhead, M., Bachmann, M., Barthès, B., Ben Dor, E., Brown, D. J., Clairotte, M., Csorba, A., Dardenne, P., Demattê, J. A. M., Genot, V., Guerrero, C., Knadel, M., Montanarella, L., Noon, C., Ramirez-Lopez, L., Robertson, J., Sakai, H., Soriano-Disla, J. M., Shepherd, K. D., Stenberg, B., Towett, E. K., Vargas, R. and Wetterlind, J.: Soil Spectroscopy: An Alternative to Wet Chemistry for Soil Monitoring, in Advances in Agronomy, vol. 132, pp. 139–159., 2015.

O'Leary, G. J., Liu, D. L., Ma, Y., Li, F. Y., McCaskill, M., Conyers, M., Dalal, R., Reeves, S., Page, K., Dang, Y. P. and Robertson, F.: Modelling soil organic carbon 1. Performance of APSIM crop and pasture modules against long-term experimental data, Geoderma, 264(November 2015), 227–237, doi:10.1016/j.geoderma.2015.11.004, 2016.

Parton, W. J., Schimel, D. S., Cole, C. V. and Ojima, D. S.: Analysis of Factors Controlling Soil Organic Matter Levels in Great Plains Grasslands, Soil Sci. Soc. Am. J., 51(5), 1173, doi:10.2136/sssaj1987.03615995005100050015x, 1987.

Parton, W. J., Scurlock, J. M. O., Ojima, D. S., Gilmanov, T. G., Scholes, R. J., Schimel, D. S., Kirchner, T., Menaut, J.-C., Seastedt, T., Garcia Moya, E., Kamnalrut, A. and Kinyamario, J. I.: Observations and modeling of biomass and soil organic matter dynamics for the grassland biome worldwide, Global Biogeochem. Cycles, 7(4), 785–809, doi:10.1029/93GB02042, 1993.

Piepho, H. P., Büchse, A. and Richter, C.: A Mixed Modelling Approach for Randomized Experiments with Repeated Measures, J. Agron. Crop Sci., 190(4), 230–247, doi:10.1111/j.1439-037X.2004.00097.x, 2004.

Poeplau, C., Don, A., Dondini, M., Leifeld, J., Nemo, R., Schumacher, J., Senapati, N. and Wiesmeier, M.: Reproducibility of a soil organic carbon fractionation method to derive RothC carbon pools, Eur. J. Soil Sci., 64(6), 735–746, doi:10.1111/ejss.12088, 2013.

Poeter, E. P., Hill, M. C., Banta, E. R., Mehl, S. and Christensen, S.: UCODE_2005 and six other computer codes for universal sensitivity analysis, inverse modeling, and uncertainty evaluation, U.S. Geological Survey Techniques and Methods 6-A11, 283p. (As updated in Feb 2008)., 2005.

Poeter, E. P., Hill, M. C., Lu, D., Tiedeman, C. R. and Mehl, S.: UCODE_2014, with New Capabilities to Define Parameters Unique to Predictions, Calculate Weights using Simulated Values, Estimate Parameters with SVD, Evaluate Uncertainty with MCMC, and More, Integrated Groundwater Modeling Center Report Number: GWMI 2014-02., 2014.

Poyda, A., Wizemann, H.-D., Ingwersen, J., Eshonkulov, R., Högy, P., Demyan, M. S., Kremer, P., Wulfmeyer, V. and Streck, T.: Carbon fluxes and budgets of intensive crop rotations in two regional climates of southwest Germany, Agric. Ecosyst. Environ., 276, 31–46, doi:10.1016/j.agee.2019.02.011, 2019.

Puttaso, A., Vityakon, P., Rasche, F., Saenjan, P., Treloges, V. and Cadisch, G.: Does Organic Residue Quality Influence Carbon Retention in a Tropical Sandy Soil?, Soil Sci. Soc. Am. J., 77(3), 1001, doi:10.2136/sssaj2012.0209, 2013.

S. Hansen, P. Abrahamsen, C. T. Petersen and M. Styczen: Daisy: Model Use, Calibration, and Validation, Trans. ASABE, 55(4), 1317–1335, doi:10.13031/2013.42244, 2012.

Segoli, M., De Gryze, S., Dou, F., Lee, J., Post, W. M., Denef, K. and Six, J.: AggModel: A soil organic matter model with measurable pools for use in incubation studies, Ecol. Modell., 263, 1–9, doi:10.1016/j.ecolmodel.2013.04.010, 2013.

Sohi, S. P., Mahieu, N., Arah, J. R. M., Powlson, D. S., Madari, B. and Gaunt, J. L.: A Procedure for Isolating Soil Organic Matter Fractions Suitable for Modeling, Soil Sci. Soc. Am. J., 65(4), 1121, doi:10.2136/sssaj2001.6541121x, 2001.

Sulman, B. N., Moore, J. A. M., Abramoff, R., Averill, C., Kivlin, S., Georgiou, K., Sridhar, B., Hartman, M. D., Wang, G., Wieder, W. R., Bradford, M. A., Luo, Y., Mayes, M. A., Morrison, E., Riley, W. J., Salazar, A., Schimel, J. P., Tang, J. and Classen, A. T.: Multiple models and experiments underscore large uncertainty in soil carbon dynamics, Biogeochemistry, 141(2), 109–123, doi:10.1007/s10533-018-0509-z, 2018.

Tinti, A., Tugnoli, V., Bonora, S. and Francioso, O.: Recent applications of vibrational mid-infrared (IR) spectroscopy for studying soil components: A review, J. Cent. Eur. Agric., 16(1), 1–22, doi:10.5513/JCEA01/16.1.1535, 2015.

Vrugt, J. A.: Markov chain Monte Carlo simulation using the DREAM software package: Theory, concepts, and MATLAB implementation, Environ. Model. Softw., 75, 273–316, doi:10.1016/j.envsoft.2015.08.013, 2016.

Wattenbach, M., Gottschalk, P., Hattermann, F., Rachimow, C., Flechsig, M. and Smith, P.: A framework for assessing uncertainty in ecosystem models, in (eds). Proceedings of the iEMSs Third Biennial Meeting: "Summit on Environmental Modelling and Software". International Environmental Modelling and Software Society, Burlington, USA, July 2006. CD ROM. Internet: http://www.iemss.org/iemss2006/sessions/all., 2006.

Wizemann, H.-D., Ingwersen, J., Högy, P., Warrach-Sagi, K., Streck, T. and Wulfmeyer, V.: Three year observations of water vapor and energy fluxes over agricultural crops in two regional climates of Southwest Germany, Meteorol. Zeitschrift, 24(1), 39–59, doi:10.1127/metz/2014/0618, 2015.

Zimmermann, M., Leifeld, J., Schmidt, M. W. I., Smith, P. and Fuhrer, J.: Measured soil organic matter fractions can be related to pools in the RothC model, Eur. J. Soil Sci., 58(3), 658–667, doi:10.1111/j.1365-2389.2006.00855.x, 2007.

https://doi.org/10.5194/bg-2019-292
Preprint. Discussion started: 7 August 2019

9 Tables

Table 1 Locations, descriptions, and initial soil organic carbon (SOC) stocks of Study Sites

Study Site	UTM Degrees Lat	UTM Degrees Long	Soil type	Depth of measurements (cm)	Clay (%)	Silt (%)	Initial SOC (%)	Bulk density (Mg/m³)	Initial SOC stocks in the measured depth (Mg/ha)	Years of bulk soil availability	Types of available measurements
Ultuna	59.821879	17.656348	Eutric Cambisol	0 - 20	37	41	1.50	1.44	43.22	1956, 79, 95, 2005	SOC, DRIFTS
Bad Lauchstädt	51.391605	11.877028	Haplic Chernozem	0 - 20	21	68	1.82	1.24	45.08	1985, 2001, 04, 08	SOC, DRIFTS
Kraichgau 1	48.928517	8.702794	Stagnic Luvisol	0 - 30	18	97	0.90	1.37	37.10	2009 - 16	SOC, DRIFTS, SMB-C
Kraichgau 2	48.927748	8.708884	Stagnic Luvisol	0 - 30	18	80	1.04	1.33	41.61	2009 - 16	SOC, DRIFTS, SMB-C
Kraichgau 3	48.927197	8.715891	Stagnic Luvisol	0 - 30	17	81	0.89	1.44	38.50	2009 - 16	SOC, DRIFTS, SMB-C
Swabian Jura 1	48.527510	9.769429	Calcic Luvisol	0 - 30	38	56	1.78	1.32	70.33	2009 - 16	SOC, DRIFTS, SMB-C
Swabian Jura 2	48.529857	9.773253	Anthrosol	0 - 30	29	68	1.95	1.38	80.85	2009 - 13	SOC, DRIFTS, SMB-C
Swabian Jura 3	48.547035	9.773176	Rendzic Leptosol	0 - 30	45	51	1.91	1.07	61.27	2009 - 13	SOC, DRIFTS, SMB-C

SOC = soil organic carbon, DRIFTS = Diffuse reflectance mid infrared Fourier transform spectroscopy, SMB-C = soil microbial biomass carbon

https://doi.org/10.5194/bg-2019-292
Preprint. Discussion started: 7 August 2019

Biogeosciences
Discussions
Open Access
EGU

Table 2 Values of the two initial parameter sets for the DAISY SOM model that were used in this study. A graphical display of pools and the most important parameters for this study is found in Figure 1.

Parameter	Default DAISY	Bruun (2003)	Unit
kSOM_slow	$2.70 * 10^{-6}$ #	$4.30 * 10^{-5}$ x	d^{-1}
kSOM_fast	$1.40 * 10^{-4}$ #	$1.40 * 10^{-4}$ #	d^{-1}
kSMB_slow	$1.85 * 10^{-4}$ *	$1.85 * 10^{-4}$ *	d^{-1}
kSMB_fast	$1.00 * 10^{-2}$ *	$1.00 * 10^{-2}$ *	d^{-1}
kAOM_slow	0.012 *	0.012 *	d^{-1}
kAOM_fast	0.05 *	0.05 *	d^{-1}
maint_SMB_slow	$1.80 * 10^{-3}$ *	$1.80 * 10^{-3}$ *	d^{-1}
maint_SMB_fast	$1.00 * 10^{-2}$ *	$1.00 * 10^{-2}$ *	d^{-1}
CUE_SMB	0.60 #	0.60 #	kg kg^{-1}
CUE_SOM_slow	0.40 *	0.40 *	kg kg^{-1}
CUE_SOM_fast	0.50 *	0.50 *	kg kg^{-1}
CUE_AOM_slow	0.13 *	0.13 *	kg kg^{-1}
CUE_AOM_fast	0.69 *	0.69 *	kg kg^{-1}
f_{SOM_slow} (humification efficiency)	0.10 #	0.30 x	kg kg^{-1}
part SMB > SOM_fast	0.40 #	0.40 #	kg kg^{-1}
fraction of SOM_slow at steady state Bruun (2002) equation	0.84	0.49	kg kg^{-1}

k = turnover rate, maint = maintenance respiration, CUE = carbon use efficiency, AOM = added organic matter (not considered in this study), part = partitioning; Source: # original Jensen (1997), * modified by Müller (1997), x modified by Bruun (2003)

https://doi.org/10.5194/bg-2019-292
Preprint. Discussion started: 7 August 2019

Table 3 Soil properties at the start and end of the bare fallow experiment at each site

Site	Start (year)	End (year)	Depth of modelled layer (cm)	Bulk density of modelled layer (t/m^3)	SOC at start t/ha	SOC at end t/ha	SMB-C at start t/ha	SMB-C at end t/ha	DRIFTS SOM in slow % at start (105°C)	DRIFTS SOM in slow % at end (105°C)	%SOM loss of initial	Number of years	%SOM loss per year of initial
Ultuna	1956	2005	0 - 20	1.44	43.22	26.51	**X**	**X**	54	91	39%	50	0.8%
Bad Lauchstädt	1983	2008	0 - 20	1.24	45.08	41.91	**X**	**X**	70	80	7%	26	0.3%
Kraichgau 1	2009	2015	0 - 30	1.37	37.10	32.59	0.847	0.408	80	98	12%	7	1.7%
Kraichgau 2	2009	2015	0 - 30	1.33	41.61	38.66	0.853	0.314	73	93	7%	7	1.0%
Kraichgau 3	2009	2015	0 - 30	1.44	38.50	35.06	0.672	0.261	76	99	9%	7	1.3%
Swabian Jura 1	2009	2015	0 - 30	1.32	70.33	63.29	1.566	0.654	64	83	10%	7	1.4%
Swabian Jura 2	2009	2013	0 - 30	1.38	80.85	79.61	1.805	0.970	66	83	2%	5	0.3%
Swabian Jura 3	2009	2013	0 - 30	1.07	61.27	70.29	1.350	0.990	61	76	-15%	5	-2.9%

X = no data available for this site

https://doi.org/10.5194/bg-2019-292
Preprint. Discussion started: 7 August 2019

Table 4. Least square means of the (backtransformed) absolute error of DAISY bare-fallow simulations for SOC and SMB-C for Ultuna, Bad Lauchstädt and Kraichgau + Swabian Jura combined. The values are the estimate for the end of the simulation period (number of years in brackets). Different capital letters indicate significant differences ($p<0.05$) within columns (not tested between sites). For Bad Lauchstädt, the initialization effect was nonsignificant, so only the least square means for the effect of the parameter set is displayed.

		Ultuna (50yr)	Bad Lauchstädt (23yr)	Kraichgau + Swabian Jura (7 yr)	Kraichgau + Swabian Jura (7 yr)
Parameter set	**Initialization**	**Least square means of errors (SOC t/ha)**	**Backtransformed least square means of errors (SOC t/ha)**	**Backtransformed least square means of errors (SOC t/ha)**	**Least square means of errors (SMB-C t/ha)**
Mueller (1997)	ratio of steady state assumption	13.91 A	2.22 A	4.50 A	0.354 A
	peak ratio of DRIFTS at 32°C	10.86 B		4.50 A	0.317 AB
	peak ratio of DRIFTS at 65°C	10.06 C		4.42 A	0.274 ABC
	peak ratio of DRIFTS at 105°C	8.52 D		4.28 A	0.205 CD
Bruun (2003)	ratio of steady state assumption	5.84 H	6.01 B	3.12 B	0.231 BCD
	peak ratio of DRIFTS at 32°C	7.06 E		3.31 B	0.179 CDE
	peak ratio of DRIFTS at 65°C	6.75 F		3.30 B	0.160 DE
	peak ratio of DRIFTS at 105°C	6.15 G		3.25 B	0.131 E

https://doi.org/10.5194/bg-2019-292
Preprint. Discussion started: 7 August 2019

Table 5 Optimized turnover rates and humification efficiency of this study using the combined site with original weighting compared to other Bayesian calibrations and standard values of commonly used models. If the temperature function was given or site temperature specified, the turnover rates were normalized with an exponential equation to 10°C which is standard in DAISY.

model	**DAISY**	**ICBM**	**CBM-CFS3**	**APSIM**	**own creation**	**CENTURY**	**DAISY**	**DAISY**
reference	**This study**	**Ahrens**	**Hararuk**	**Luo**	**Clifford**	**Parton**	**Mueller**	**Bruun**
year	**2019**	**2014**	**2017**	**2016**	**2014**	**1993**	**1997**	**2003**
turnover rates of the fast pool (recalculated to d^{-1} at 10°C)								
minimum	$1.07 * 10^{-4}$	$4.57 * 10^{-4}$	$6.30 * 10^{-4}$	NA	NA - no			
optimum	$2.07 * 10^{-4}$	$4.57 * 10^{-3}$	$1.97 * 10^{-4}$	NA	temperature	$9.32 * 10^{-5}$	$1.40 * 10^{-4}$	$1.40 * 10^{-4}$
maximum	$3.27 * 10^{-4}$	$2.28 * 10^{-2}$	$1.05 * 10^{-3}$	NA	found			
turnover rates of the slow pool (recalculated to d^{-1} at 10°C)								
minimum	$2.99 * 10^{-6}$	$4.57 * 10^{-7}$	$9.86 * 10^{-6}$	$1.00 * 10^{-4}$	$1.10 * 10^{-4}$			
optimum	$3.11 * 10^{-5}$	$2.28 * 10^{-5}$	$1.10 * 10^{-5}$	$3.00 * 10^{-4}$	$1.67 * 10^{-4}$	$2.10 * 10^{-6}$	$2.70 * 10^{-6}$	$4.30 * 10^{-5}$
maximum	$6.14 * 10^{-5}$	$4.57 * 10^{-5}$	$1.32 * 10^{-5}$	$6.00 * 10^{-4}$	$2.19 * 10^{-4}$			
portion of fast to slow pool (humification efficiency)								
minimum	0.05	0.05						
optimum	0.3	0.2				0.3	0.1	0.3
maximum	0.35	0.35						

References: (Ahrens et al., 2014; Bruun et al., 2003; Clifford et al., 2014; Hararuk et al., 2017; Luo et al., 2016; Mueller et al., 1997; Parton et al., 1993)

https://doi.org/10.5194/bg-2019-292
Preprint. Discussion started: 7 August 2019

Biogeosciences
Discussions
Open Access
EGU

10 Figures

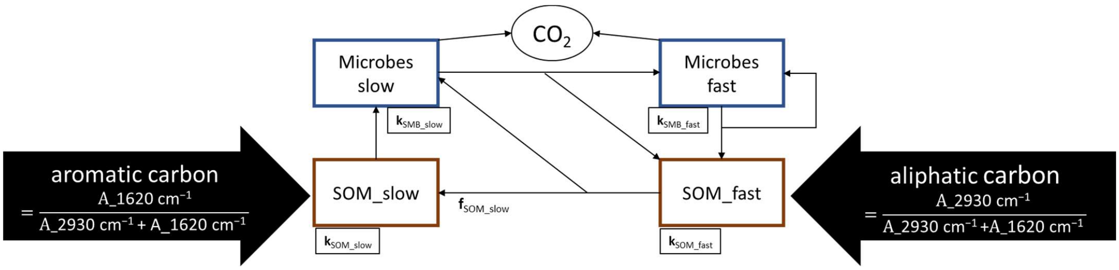

Figure 1 Original structure of the internal cycling of SOM in the DAISY model, as it was used in this study. A_XXXX cm^{-1} is the area of each peak obtained by DRIFTS, kSOM and SMB are turnover rates of the pools and fSOM is the humification efficiency. Other parameters are found in Table 2.

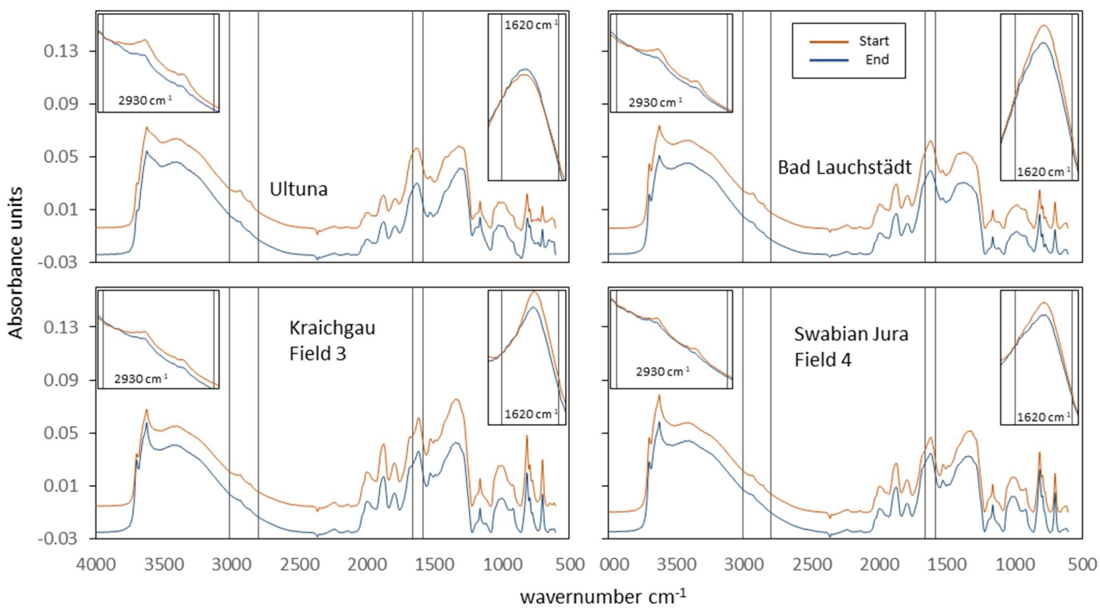

Figure 2 DRIFTS baseline corrected and vector normalized example spectra of bulk soil samples (dried at 105°C) of the first and last year of the bare fallow plots at four sites. Fallow periods were 50 years (Ultuna), 24 years (Bad Lauchstädt) and 7 years (Kraichgau and Swabian Jura). Small pictures on the top left and right, are zoomed versions of the 2930cm^{-1} peak and the 1620cm^{-1} peak, respectively. More details on the sites in Table 3.

https://doi.org/10.5194/bg-2019-292
Preprint. Discussion started: 7 August 2019

Biogeosciences
Discussions
Open Access

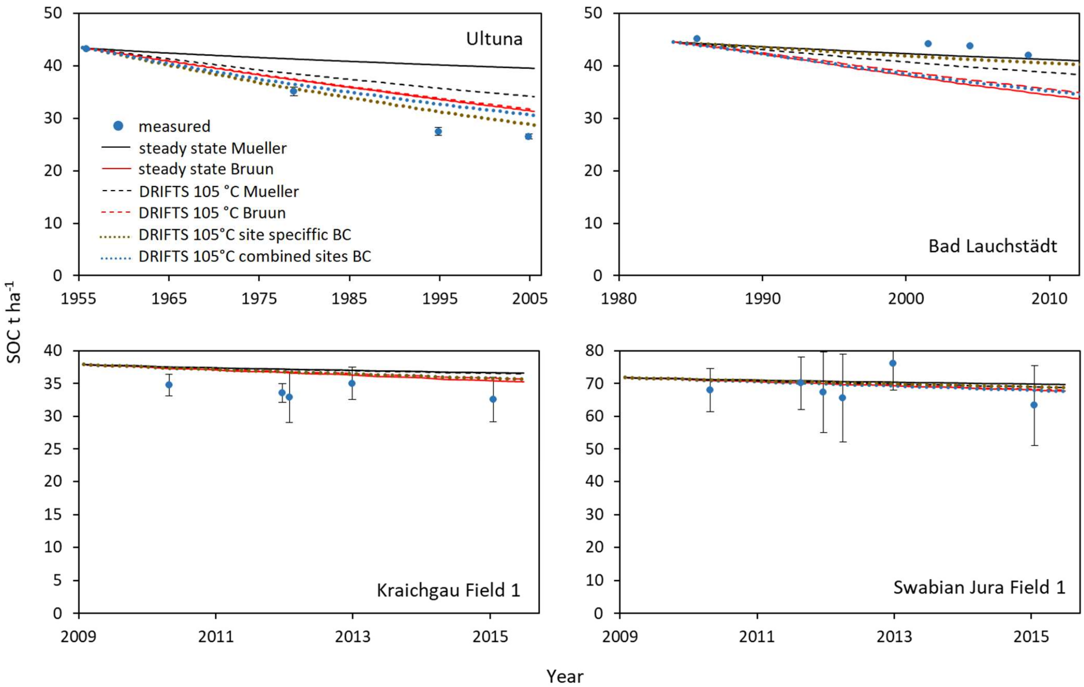

Figure 3 Example of SOC simulations from Ultuna (top left), Bad Lauchstädt (top right), Kraichgau field 1 (bottom left) and Swabian Jura Field 1 (bottom right). Initializations were done (i) assuming steady state using the formula of Bruun and Jensen, (2002) (equation 1) with both turnover rates of Mueller et al., (1997) and Bruun et al., (2003) and (ii) by the ratio of the 2930 cm^{-1} to the 1620 cm^{-1} peak of DRIFTS spectra at 105°C drying temperature using both turnover rates for simulations (simulations using the other drying temperatures for DRIFTS in the supplementary). The site specific and the combination of all sites Bayesian calibrations (BC) are also displayed. Bars indicate standard deviation of all plots per field.

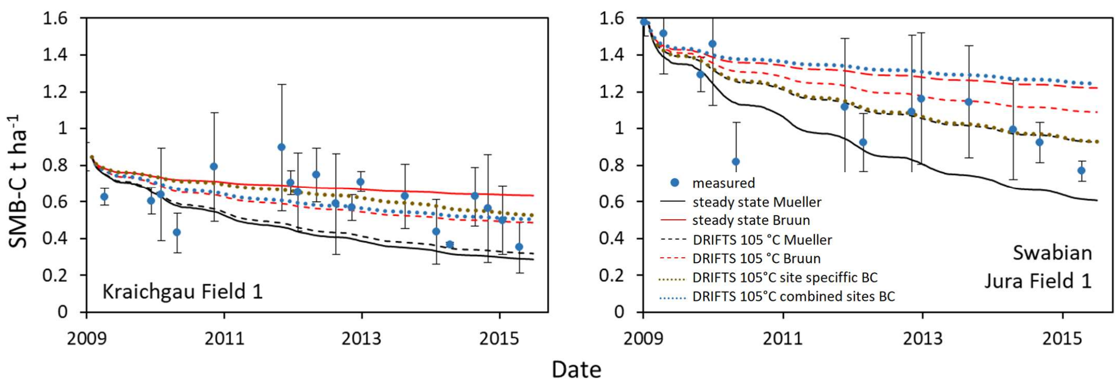

Figure 4 Example SMB-C simulations from Kraichgau field 1 (left) and Swabian Jura Field 1 (right). Initializations were done (i) assuming steady state using the formula of Bruun and Jensen, (2002) with turnover rates of Mueller et al., (1997) and Bruun et al., (2003) and (ii) by the ratio of the 2930 cm^{-1} to the 1620 cm^{-1} peak of DRIFTS spectra at 105° C drying temperature using both turnover rates for simulations (simulations using the other drying temperatures for DRIFTS in the supplementary). The site specific and the combination of all sites Bayesian calibrations (BC) are also displayed. Bars indicate standard deviation of all plots per field.

https://doi.org/10.5194/bg-2019-292
Preprint. Discussion started: 7 August 2019

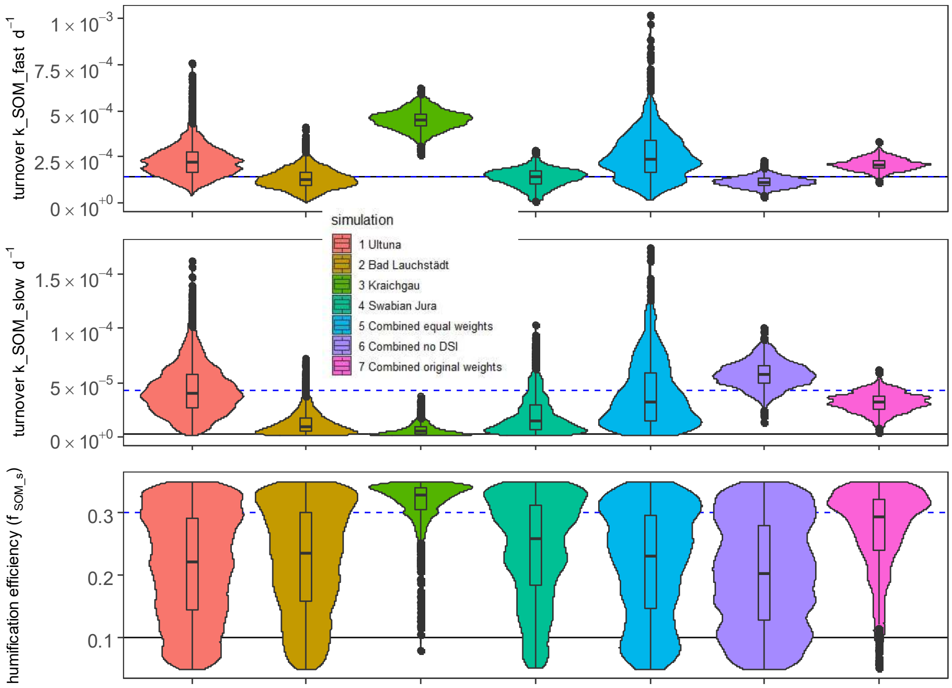

Figure 5 Violin plots of the parameter distributions, obtained by the Bayesian calibration using only the individual sites (1-4) and all sites combined (5-7) with different weighing schemes. The black line corresponds to the parameters of Mueller (1997), the blue dashed line to the parameters of Bruun (2003).

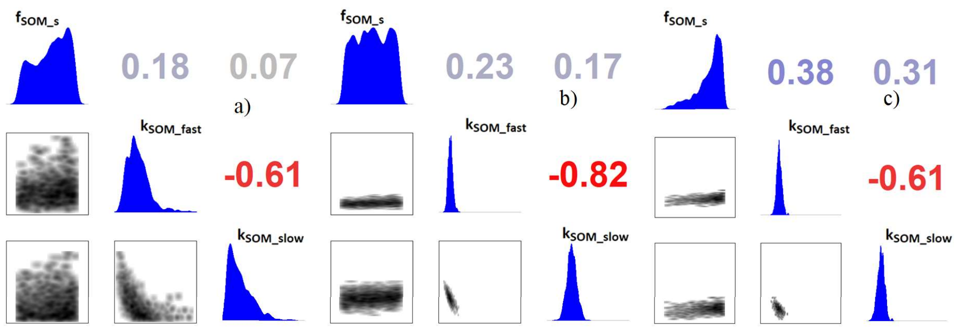

Figure 6 Correlation matrices of posterior distributions from the Bayesian calibrations of a) All combined with equal weights using the DSI b) All combined with original weights without DSI and c) All combined with original weights using the DSI. The plots of the rest of the simulations can be found in the supplemental material.

https://doi.org/10.5194/bg-2019-292
Preprint. Discussion started: 7 August 2019

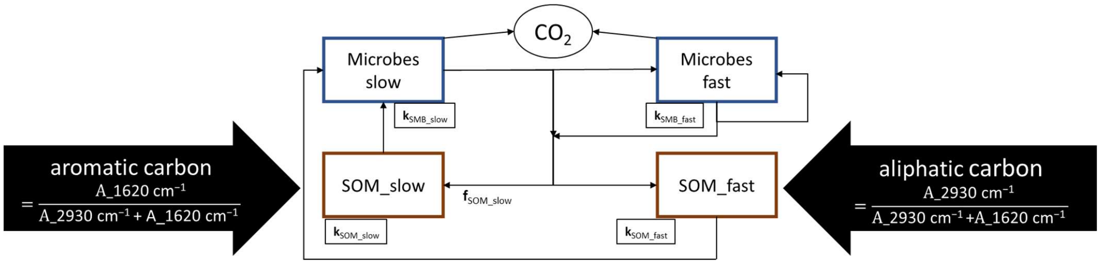

Figure 7 Suggested improvements to the internal cycling structure of SOM in the DAISY model. The division into fast and slow cycling SOM, corresponding to aliphatic and aromatic carbon happens at the death of microbes. Aliphatic carbon no longer becomes complex carbon without the involvement of microbes.